Anatomical Science International (2024) 99:268–277
https://doi.org/10.1007/s12565-024-00766-6

ORIGINAL ARTICLE

Age-related changes in densitometry and histomorphometry of long bone during the pubertal growth spurt in male rats

Kiyoung Ryu[1] · **Okto Lee**[2] · **Jaesook Roh**[2]

Received: 1 January 2024 / Accepted: 9 March 2024 / Published online: 10 April 2024

Abstract

Because experimental studies to determine the developmental toxicity of exposure to various substances in children are impossible, many studies use immature male rats. This study aimed to provide normative data for longitudinal bone growth with age during the puberty in male rats. In order to evaluate long bone growth and mineralization we examined bone size and bone density by dual-energy X-ray absorptiometry, analyzed histomorphometry of the growth plate, and serum hormone levels relevant to bone growth from postnatal day (PD)20 to PD60. The length and weight of long bones increased strongly by PD40, and no further increase was observed after PD50. On the other hand, tibial growth plate height decreased sharply after PD50 along with a reduction in the number of cells and columns, which was probably responsible for the absence of further lengthening of long bones. Parameters related to bone formation such as bone area ratio, and the thickness and number of trabeculae, also increased significantly between PD40 and PD50. Furthermore, serum levels of IGF-1 peaked at PD30 and testosterone increased rapidly on and after PD40, when IGF-1 levels were going down. These changes may participate in the parallel increase in mineral acquisition, as well as lengthening of long bones. Our findings provide comprehensive data for changes in bone density, histomorphometry of long bones, and hormone levels relevant to bone growth during the growth spurt. This will be useful for planning animal toxicological studies, particularly for deciding on the appropriate age of animals to use in given experiments.

Keywords Densitometry · Growth plate · Histomorphometry · Long bone · Puberty

Introduction

With the recent industrial development, exposure to various environmental substances increases. Although many clinical trials have been conducted to examine the potential developmental toxicity of various substances, experimental studies aimed at children are ethically impossible. Thus, the rat is widely used as an excellent animal model for biomedical research because of its small size, relatively low cost, rapid reproduction rate, and similarity of its many skeletal characteristics with human (Waynforth and Flecknell 1980; Zoetis et al. 2003). Experiments on the effect of various substances on bone growth can yield different results because of differences in growth rate depending on the age and sex of rats (Hansson et al. 1972). Therefore, careful selection of the appropriate age is crucial. For instance, peripubertal rats are required for studying long bone growth. Puberty, when physical growth accelerates and more than 15% of adult height is achieved (Cutler 1997), is vulnerable to many insults (Gluckman and Hanson 2006). Similarly, the rapid increase in estrogen during puberty in female rats causes the bone growth plates to close earlier than in males and increases individual variation (Börjesson et al. 2010; Hansson et al. 1972). Therefore, the majority of toxicologists use male rats to study long bone growth rather than females, which are subject to the periodic effects of estrogen (Wheeler 1991).

Although earlier investigators of long bone growth used various parameters to measure growth in experimental animals, no study showed hormonal changes associated with bone growth combined with the histomorphometric changes in long bones during puberty in rats. The current study was designed to provide the detailed age-dependent changes in

✉ Jaesook Roh
rohjaesook@hanyang.ac.kr

[1] Department of Obstetrics & Gynecology, College of Medicine, Hanyang University, Guri 11923, South Korea

[2] Laboratory of Reproductive Endocrinology, Department of Anatomy & Cell Biology, College of Medicine, Hanyang University, Seoul 133-791, South Korea

densitometry and histomorphometry of the long bones during the pubertal growth spurt. In order to evaluate changes in bone density and long bones in relation to age we analyzed densitometry and histomorphometry of the growth plate, and long bone size throughout most of the growth spurt. In addition, serum levels of hormones such as IGF-1, estradiol, and testosterone, known to be important in the pubertal growth spurt, were evaluated.

Materials and methods

Animals

Two-week old male Sprague–Dawley rats were obtained with their mothers from Samtako Biokorea (Osan, South Korea) and were allowed to acclimate under controlled humidity, temperature and light conditions. Animal care was consistent with institutional guidelines, and the Hanyang University ACUC committee approved all procedures involving animals (HY-IACUC-2020-0085A). All animals were weaned from their mothers at 21 days of age and fed standard rat chow ad libitum. Postnatal days (PD) 20–60 were selected to cover the time of rapid skeletal growth during puberty (Hansson et al. 1972; Walker and Kember 1972). A total of 30 rats were assigned at random to 5 groups (N = 6/group) and killed following protocols and ethical procedures on PD20, 30, 40, 50, and 60, respectively. They were anesthetized with isoflurane inhalation (Forane solution, Choongwae Pharma. Corp., Seoul, Korea) and killed by cervical dislocation under deep anesthesia. Terminal blood samples were collected by heart puncture and serum samples were obtained for hormone analysis.

Dual-energy X-ray absorptiometry

The body composition of all animals was evaluated on day before they were killed by dual-energy X-ray absorptiometry (DXA)(Discovery W QDR series, Hologic Inc., Bedford, MA, USA), using the small animal software package. This software had been validated also as an excellent noninvasive technique for measuring bone in very young animals (Engelbregt et al. 1999). Bone mineral content (BMC, g) and bone mineral density (BMD, g/cm^2) of the lumbar vertebrae, and both femora and tibiae were analyzed. Animals were anesthetized by isoflurane inhalation during examination.

Preparation of femora and tibiae

To analyze long bone growth with age, both leg bones (femora and tibiae) were dissected from each rat, and cleaned of soft tissue at necropsy. They were then weighed and their lengths measured; for femur lengths from the proximal end of the femur to the distal end with the bone placed parallel to the ruler, and for tibia lengths from the top of the plateau to the bottom of the lateral malleolar process with a precision digital caliper (± 0.03 mm) (NA500-150S, Bluebird, China) as described by Weinreb et al. (1991).

Tissue processing and histomorphetric analysis

In this study, tibiae were chosen for histomorphometric analyses because they are the longest bones. Both tibiae were fixed in 10% buffered formalin for 48 h. They were decalcified in a solution containing EDTA in 0.1 M Tris at 4 ℃, which was replaced weekly until decalcification was complete. They were then cut in half longitudinally with a razor blade, dehydrated in a graded ethanol series, cleared in chloroform, and embedded in paraffin. Serial longitudinal Sections. (5 µm thickness) were obtained from the proximal part of the tibiae using a rotation microtome (RM 2155 Autocut; Leica, Heidelberg, Germany) with a tungsten carbide blade and stained with Alcian blue to stain cartilage matrix. All histomorphometric evaluations were performed by the same trained, calibrated and blinded examiner, using an image analysis system (Leica LAS software) coupled to a light microscope (DM4000B, Leica, Heidelberg, Germany) with final magnifications of 50-, 100- or 200-fold.

The overall height of the growth plate (GP) cartilage is used to assess longitudinal bone growth quantitatively (Hunziker and Schenk 1989; Roach et al. 2003). As previously described (Choi et al. 2016), the GP is divided into three layers, the resting zone (RZ), proliferative zone (PZ), and hypertrophic zone (HZ) (Suppl. Fig. S1A), and we analyzed the PZ and HZ, which are actively involved in the synchronized processes of chondrogenesis resulting in longitudinal bone growth (Hunziker 1994). The heights of each zone and the overall GP, and the numbers of cells, were measured with image analysis software (Leica LAS software). The averages of 20 GP measurements (4 serial sections per animal, 5 measurements per section) were obtained for each tibia at 100-fold magnification, and combined to obtain a mean value per animal. The number of chondrocytes in the PZ and HZ were counted within the same defined region (0.3 mm^2) at 200-fold magnification, and the mean of 8 measurements was calculated for each tibia.

For the metaphysis, 16 measurements per tibiae were made of the heights of the whole, primary (1°), and secondary (2°) spongiosa (Sn) at 50-fold magnification (Suppl. Fig.S1B). The 1° Sn is located under the GP and characterized by thin trabeculae with a calcified cartilage core covered with bone (Hunziker and Schenk 1989). As the 1° Sn is not suitable for histomorphometric analysis due to the inhomogeneity of bone structure resulting from growth processes (Hunziker and Schenk 1989), a more detailed examination was performed in the whole 2° Sn,

with its homogeneous bone tissue. The 2° Sn, which is located under the 1° Sn and characterized by a network of larger trabeculae (extending 1–1.9 mm distal to the epiphyseal GP). For the analysis of the 2° Sn, whole fields of vision on four consecutive Alcian blue-stained sections of each tibiae were evaluated at 100-fold magnification. All the standardized terms used in trabecular bone analysis are based on standard histomorphometry (Parfitt et al. 1987). The areas of trabecular bone within a reference area (1.229 mm^2) of the proximal tibiae were measured with the aid of a summagraphics digitizer interfaced with a Compaq computer on printed copies by point counting using a square lattice (0.3 mm) (Suppl. Fig. S1C). Trabeculae in contact with the cortices were excluded from the measurements as described by Parfitt et al. (1987). Data are presented as the ratio of trabecular bone area to tissue area. Trabecular width (Tb.Wi) (μm), number (mm^{-1}) and separation (μm) were calculated according to stereological formulas described in a previous report (Choi et al. 2016). Averages were calculated from the data for each animal; they were pooled and a mean value was calculated for each group.

Hormone measurements

Serum hormone levels were analyzed in the serum samples taken from all animals at the end of the experiment. Insulin-like growth factor-1 (IGF-1), estradiol (E_2), and testosterone (T) were measured with commercially available enzyme-linked immunosorbent assay (ELISA) kits (Cusabio Biotech Co., LTD., China). Intra- and inter-assay coefficients of variance for IGF-1 (8, 10%), and the other hormones were ≤ 15%. Under our conditions, the limits of detection were 0.156 ng/ml for IGF-1, 15 pg/ml for E_2, and 0.06 ng/ml for T. Absorbances were read within 15 min at 450 nm against a blanking well in an ELISA Reader (BioRad, Hercules, CA). All assays were run in duplicate and each ELISA was performed twice.

Statistical analysis

Data for each group are expressed as means with standard deviations (SD). All data were analyzed using IBM SPSS Statistics 25.0 for Windows (IBM Co., Armonk, NY, USA). Jonckheere-Terpstra tests (J-T) (nonparametric test) were conducted to determine the significance of trends with age for each parameter. In addition, incremental percentages and 95% confidence intervals were calculated for differences between ages, which are being expressed as a percentage of the value of previous age. Significance was accepted at $p < 0.05$.

Results

Bone mineral status in growing rats measured by DXA

BMC and BMD were measured in lumbar vertebrae, femora and tibiae at each designated time point. The data are summarized in Fig. 1. The BMCs and BMDs of all measured regions tend to significantly increased with age (J-T, $p < 0.001$) (Suppl. Table S1). The BMCs of all measured regions increased significantly between PD20 and PD30, and again between PD30 and PD40 ($p < 0.05$) (Fig. 1A). Unlike those of other regions, the BMC of tibiae also increased significantly between PD40 and PD50 ($p < 0.05$). On the other hand, the areal BMDs of all regions increased at a relatively constant rate from PD20 to PD50, the rate of increase declined after PD50, and no increase at all was noted in the areal BMD of either tibia after PD50 (Fig. 1B).

The weight and length of long bones

To measure the growth of long bones, the weights and lengths of femora and tibiae were determined. All parameters displayed a significant increasing trend with age (J-T, $p < 0.001$) (Suppl. Table S1). There was a rapid and significant increase in weight of femora between PD20 and 30 ($p < 0.05$) but no increase in tibiae. Both weights increased between PD30 and 40 ($p < 0.05$) but the increases stagnated after PD40 (Fig. 1C). On the other hand, the lengths of both femora and tibiae increased at a relatively constant rate from PD20 to PD50, the rate of increase declined after PD50 (Fig. 1D).

Histomorphometric changes in the growth plate of the proximal tibiae with age

Histomorphometric parameters of the GP based on examination of histological sections of the proximal tibiae are depicted in Fig. 2. Representative sections of the GP are shown in Fig. 3. GP heights tend to significantly decreased with age (J-T, $p < 0.01$) (Fig. 2A, B) (Suppl. Table S2). Total GP height (μm) decreased progressively with age and a sharp reduction was noted between PD50 and PD60 (41% decrement) (Figs. 2A and 3D, E) (Suppl. Table S2). A similar change was also noted in PZ and HZ heights, and there was a particularly marked decrease in HZ height from PD50 to PD60 (59% decrement). Although PZ height also decreased profoundly between PD50 and PD60 (26% decrement), its decline was only about half of that in HZ height.

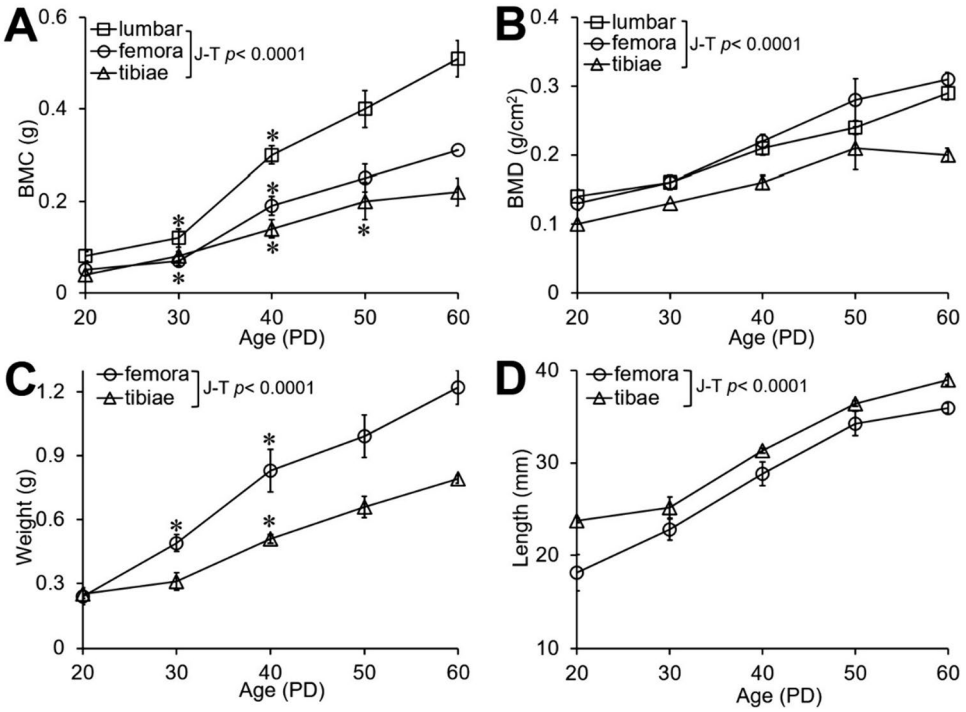

Fig. 1 Changes of bone minerals, and weights and lengths of leg bones with age. **A**, **B** Bone mineral contents (g) and density (g/cm^2) determined by dual-energy X-ray absorptiometry in lumbar, femora and tibiae. **C**, **D** Weight (g) and length (mm) of femora and tibiae. Values are mean ± SD measured in six rats. PD, postnatal day; BMC, bone mineral content; BMD, bone mineral density; open square, lumbar; open circle, femora; open triangle, tibiae. For the significance of differences between ages for each parameter, incremental percentage with 95% confidence interval are calculated; *$p < 0.05$ vs. the value of previous age (Suppl. Table S1). J-T p values indicate the significance of trends with age for each parameter analyzed with Jonckheere-Terpstra test (trend test); significance at $p < 0.05$

As a consequence, the ratio of PZ to GP was reversed and exceeded the ratio of HZ to GP at PD60 (Fig. 2B). The number of cells in the PZ and HZ displayed a significant decreasing trend with age (J-T, $p < 0.01$) (Fig. 2C, D) (Suppl. Table S2). The PZ is formed of columns of rapidly dividing chondrocytes resembling stacks of coins (Fig. 3) (Suppl. Fig. S1A). The number of cells within the defined region or number of cells per column in the PZ fluctuated up to PD40 and then fell between PD50 and PD60 (43%, 27% decrement, respectively). The number of cells within the defined region or number of cells per column in the HZ underwent similar changes with age to those in the PZ (27%, 34% decrement, respectively) (Fig. 2C, D) (Suppl. Table S2). Taken together, these findings show that the profound reduction in GP height at PD60 was accompanied by significant decreases in the numbers of cells in the PZ and HZ.

Histomorphometry of cancellous bone in the proximal tibiae

In contrast to GP height, whole Sn height did not change to PD40 but then increased between PD40 and PD50 (55% increment) ($p < 0.05$) (Fig. 2E) (Suppl. Table S2); 2° Sn heights also increased by PD50 along with all parameters related to bone formation, whereas 1° Sn heights increased between PD20 and PD30 (66% increment) ($p < 0.05$), then remained relatively constant. As a result, the percentage of 1° Sn to the whole continuously decreased after PD30 and the percentage of 2° Sn to the whole steadily increased by PD60 (Fig. 2F). The indices of trabecular bone formation analyzed mainly in the 2° Sn are summarized in Table 1 and representative sections of the 2° Sn are presented in Fig. 4. As shown in Fig. 4, the micro-architecture of the 2° Sn was markedly changed at PD50, with an increase in bone area, bone perimeter, bone area ratio and trabecular number, and, as a consequence, a decreased trabecular separation. Overall, trabecular bone formation reached a significant level at PD50, and after that, all parameters except trabecular separation decreased.

Hormone measurements

Serum levels of IGF-1, E_2 and T are depicted in Fig. 5. IGF-1 increased strongly between PD20 and PD30 ($p < 0.05$), and fell sharply by PD40 (Fig. 5A). E_2 levels were relatively constant (Fig. 5B), whereas T levels displayed a significant increasing trend with age (J-T, $p < 0.01$) and sharply rose from PD40 and peaked at PD60 ($p < 0.05$) (Fig. 5C).

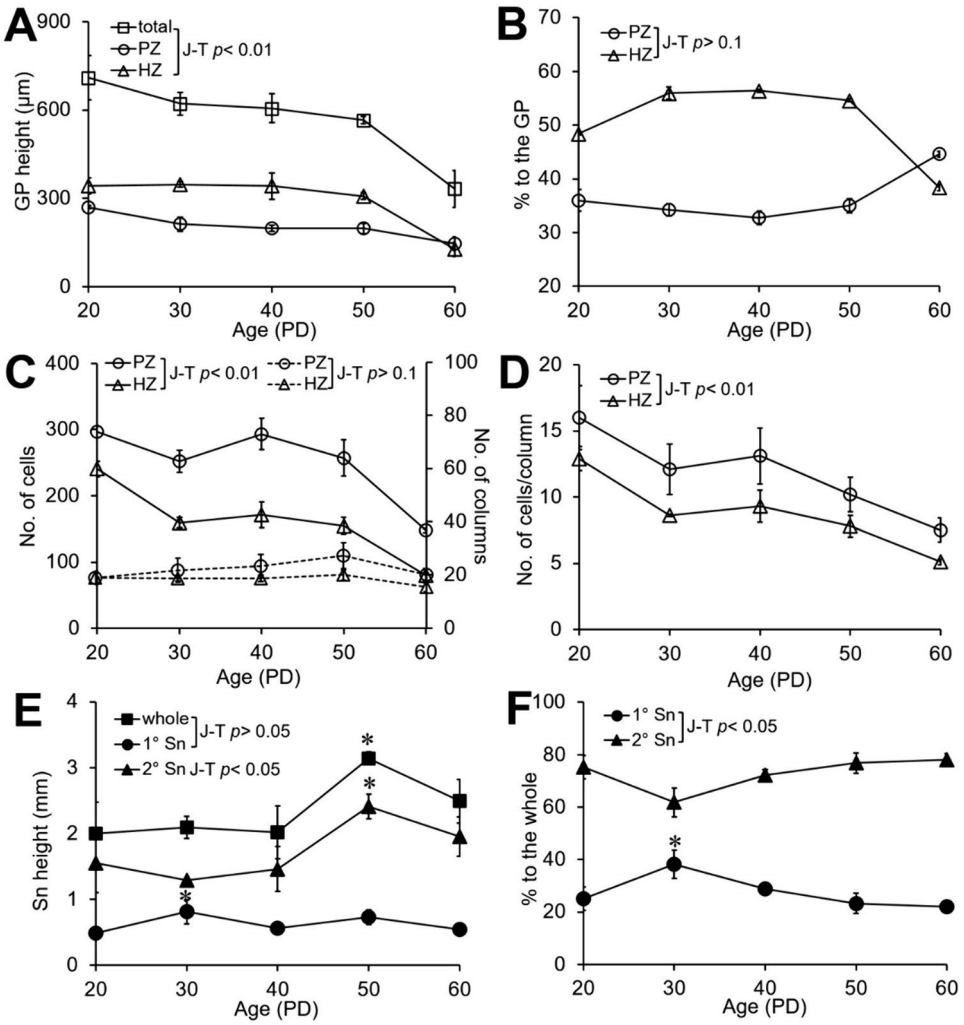

Fig. 2 Growth plate parameters analyzed from the proximal tibiae with age. **A** The heights of the total growth plate, PZ and HZ are the longitudinal dimension of the structure parallel to the long axis of the bone. **B** Percentages of the heights of PZ and HZ to the total GP. **C** Number of cells (solid line) and columns (dotted line) are mean value of 8 measurements of both tibiae counted within the same defined region (0.3 $mm.^2$) at 200-fold magnification. **D** Cell numbers per column for the PZ and HZ are mean numbers of cells in a single column spanning the longitudinal diameter of the zone. **E** The heights of the whole, 1° and 2° Sn are the longitudinal dimension of the structure parallel to the long axis of the bone. **F** Percentages of the heights of the 1° Sn and the 2° Sn to the whole Sn. Values represent means ± SD for both tibiae of six rats. PD, postnatal day; GP, growth plate; PZ, proliferative zone; HZ, hypertrophic zone; open square, total; open circle, PZ; open triangle, HZ; Sn, spongiosa; closed square, whole; closed circle, 1° Sn; closed triangle, 2° Sn. For the significance of differences between ages for each parameter, incremental percentage with 95% confidence interval are calculated; $*p < 0.05$ vs. the value of previous age (Suppl. Table S2). J-T p values indicate the significance of trends with age for each parameter analyzed with Jonckheere-Terpstra test (trend test); significance at $p < 0.05$

Discussion

Skeletal growth is one of the most striking characteristics of puberty. Although earlier investigators of long bone growth used various parameters to measure growth in experimental animals, there has been few combined study with the changes of both the weight and length of long bones, and hormones during puberty in rats. In this study, we showed the growth of long bones such as femora and tibiae in male rats from PD20 to PD60. The rate of growth of long bone was highest between PD20 and PD40, after which it slowed considerably. Significant increase in femora length began from PD20, and tibiae length began 10-day later than femora length (Fig. 1D).

These differences are consistent with other findings (Hansson et al. 1972; Lindahl 1967). The weights of femora and tibiae followed the same patterns of increases as those of length. Our results should provide a standard for the changes in long bone length and weight during the pubertal growth spurt. Adolescence is the period when the greatest bone

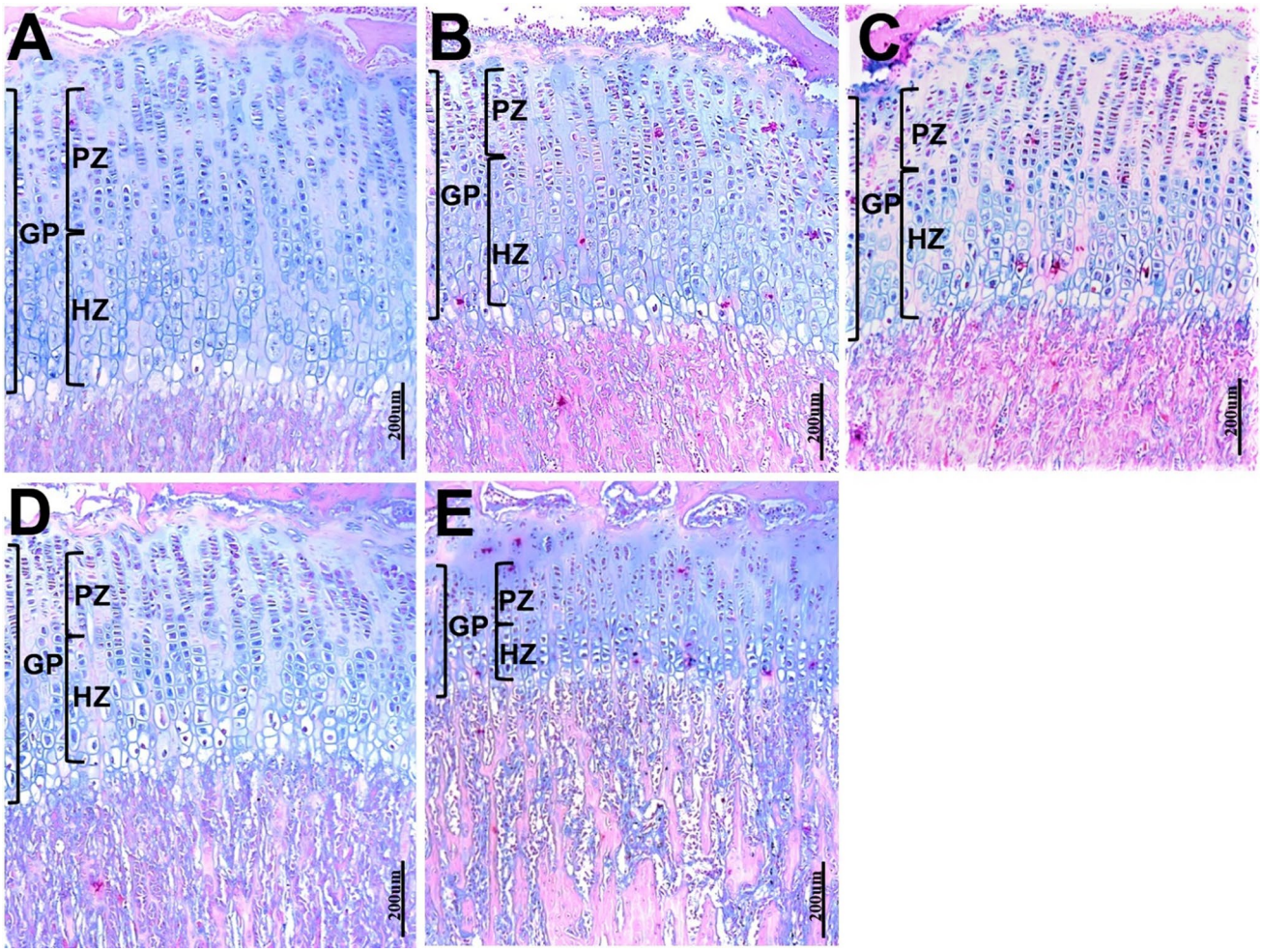

Fig. 3 Representative sections of the proximal tibia growth plate. Tissues were stained with Alcian blue, which stains collagen blue. Growth plates at **A** PD20, **B** PD30, **C** PD40, **D** PD50, and **E** PD60. The heights of the total GP, PZ and HZ are indicated. PZ, proliferative zone; HZ, hypertrophic zone. Bar = 200 μm

Table 1 Histomorphometric parameters of the cancellous bone analyzed from the 2° spongiosa of proximal tibiae

Age (PD)	20 (N = 6)	30 (N = 6)	40 (N = 6)	50 (N = 6)	60 (N = 6)	J-T *p-value*
B.Ar (mm^2)	0.19 ± 0.00	0.19 ± 0.04	0.20 ± 0.03	0.31 ± 0.04*	0.22 ± 0.05	0.188
B. Peri (mm)	16.7 ± 1.37	12.6 ± 0.92	11.5 ± 1.96	17.1 ± 1.59*	11.9 ± 1.20	0.265
B.Ar/T.Ar	15.7 ± 0.17	15.5 ± 2.89	16.3 ± 2.64	25.2 ± 3.23*	18.1 ± 4.46	0.188
Tb.Wi (μm)	23.3 ± 2.11	30.0 ± 3.56	34.8 ± 0.66	36.3 ± 3.62	37.1 ± 5.95	0.002
Tb.N (mm^{-1})	6.6 ± 0.71	5.1 ± 0.37	4.7 ± 0.80	7.0 ± 0.65*	4.8 ± 0.49	0.311
Tb.Sp (μm)	123.8 ± 9.6	165.3 ± 17.4	182.6 ± 34.4	108.2 ± 13.3	170.9 ± 6.3*	0.478

Values are means ± SD for both tibiae of six rats at each designated time point. Measurements of height represent the longitudinal dimensions of structures parallel to the long axis of the bone. Whole fields of vision on four consecutive Alcian blue-stained sections of each tibia per animal were evaluated at 100-fold magnification for the analysis of secondary spongiosa

PD postnatal day, *Sn* spongiosa, *B. Peri* bone perimeter, *B.Ar/T.Ar* trabecular bone volume, *Tb.Wi* trabecular width (thickness), *Tb.N* trabecular number, *Tb.Sp* trabecular separation

p values indicate the significance of trends with age for each parameter analyzed with Jonckheere-Terpstra test (trend test); significance at $p < 0.05$. Percentage changes between designated time points are calculated as [(Final value – Original value)/Original value] × 100% and significance is based on 95% confidence intervals (Table S2);

*$p < 0.05$ vs. the value of previous age

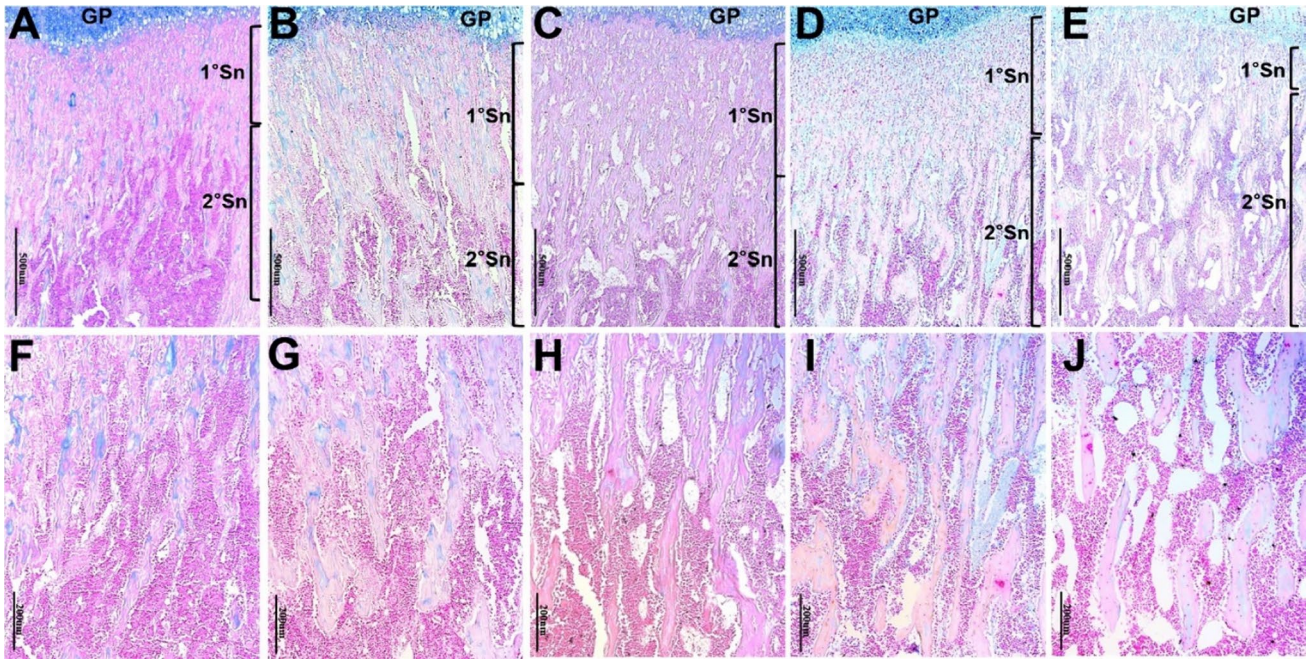

Fig. 4 Representative sections of the proximal tibia cancellous bone. Tissues were stained with Alcian blue. **A**–**E** Sections including primary and secondary spongiosa at 50-fold magnification, and **F**–**J** sections showing a part of the secondary spongiosa at 100-fold magnification. **A**, **F** PD20, **B**, **G** PD30, **C**, **H** PD40, **D**, **I** PD50, and **E**, **J** PD60. GP, growth plate; 1° Sn, primary spongiosa; 2° Sn, secondary spongiosa. Bar = 500 μm for (A–E) and 200 μm for (F–J)

mass accrual occurs (Theintz et al. 1992). BMC increased progressively with age, but its rate of increase was not homogeneous even within the leg bones; instead there was an abrupt increase of BMC in femora between PD30 and PD40, whereas the rate of increase of BMC in tibiae was roughly constant to PD50 (Fig. 1A). The age at which peak bone mass is attained in humans also differs with the site (Krabbe et al. 1979; Theintz et al. 1992). Thus, depending on the purpose of the experiment, this should be taken into consideration when deciding age of the rat and bones to analyze.

The GP is an important region of longitudinal bone growth due to endochondral ossification (Ortega et al. 2004), and its height has been employed as a measure of growth (Hunziker 1994). GP height in rats is reported to be greatest between PD20 and PD40, and to progressively decrease after PD56 (Roach et al. 2003). Similarly, we found that maximal GP expansion was achieved at PD20 and then decreased considerably, with a strong decline between PD50 and PD60 (Figs. 2A and 3). The stages of proliferation and hypertrophy are the most important for long bone growth in all three zones of the GP (Staines et al. 2013), and the gradual decline in GP height is associated with reduced height of the PZ and HZ (Weise et al. 2001). We noted a rapid drop in GP height between PD20 and PD30 mostly due to loss of the PZ, as well as a profound reduction between PD50 and PD60. In contrast, it has been reported that PZ height is constant from PD21 to PD91 in male Wistar rats (Walker and Kember 1972). Therefore, differences in strain are also one of factors to be considered before conducting the experiment.

Although linear growth can be modulated by changes in cell proliferation, cell hypertrophy is known to be a much faster and efficient way of rapidly extending columnar units (Hunziker and Schenk 1989). For instance, an increase in chondrocyte height is responsible for 44– 59% of long bone growth in rats, with the remainder due to matrix synthesis and chondrocyte proliferation (Wilsman et al. 1996). In this study, the height of the HZ was relatively constant up to PD50 and then fell greatly by PD60. Thus, the decline of GP height between PD20 and PD30 is due mainly to loss of the PZ, whereas the decline between PD50 and PD60 is due to loss of both the PZ and HZ, resulting from simultaneous decreases in cell numbers (Fig. 2). Given the fact that the chondrocytes believed to represent the functional units for longitudinal growth (Kember 1983; Lindahl 1967), the simultaneous decreases in cell numbers in the PZ and HZ point to a gradual decrease in growth fraction that already begins at PD30 (Fig. 2). Thus, the peak heights of PZ and HZ appear to occur at about PD20 when the GP is fully formed in male rats and active growth is in progress. In fact, the relatively constant height of the HZ from PD40 on could be accounted for by continuous transition of cells from the PZ and its replenishment from the RZ during the growth spurt. In agreement with previous studies (Hunziker and Schenk 1989; Roach et al. 2003; Walker and Kember 1972),

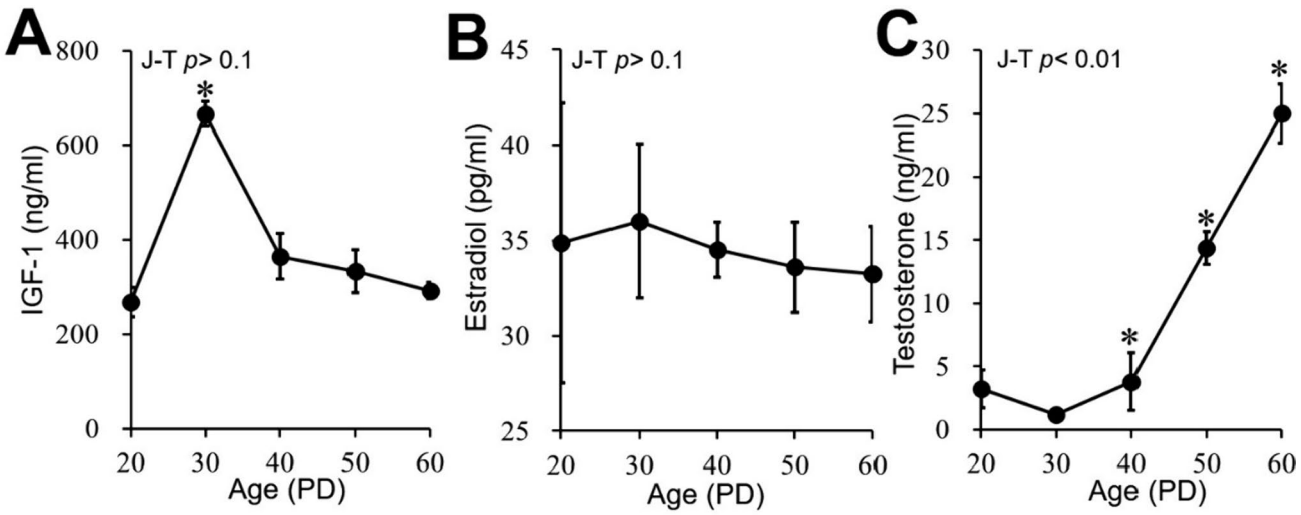

Percentage change of serum hormones levels

Age	PD20 to PD30	PD30 to PD40	PD40 to PD50	PD50 to PD60	J-T *p-value*
IGF-1	148 (0.806, 2.158)*	-45 (-1.099, 0.196)	-9 (-0.334, 0.159)	-12 (-0.421, 0.174)	0.418
Estradiol	3 (-1.110, 0.176)	-4 (-0.210, 0.126)	-3 (-0.157, 0.105)	-1 (-0.095, 0.073)	0.418
Testosterone	-64 (-1.451, 0.180)	226 (0.909, 3.605)*	279 (1.002, 4.577)*	74 (0.383, 1.089)*	0.001

Values are given as percentage change between each designated time point and values in the parentheses indicate 95% confidence interval. *p< 0.05. The percentage change is calculated by [(Final value – Original value)/Original value] × 100%. J-T p values indicate the significance of trends with age for each parameter analyzed with Jonckheere-Terpstra test (trend test); significance at p< 0.05.

Fig. 5 Serum levels of **A** IGF-1, **B** Estradiol and **C** Testosterone with age. Data are presented as mean ± SD measured in six rats per group at each designated time point, based on two independent measurements. PD, postnatal day. For the significance of differences between ages for each parameter, incremental percentage with 95% confidence interval are calculated (lower panel); *$p < 0.05$ vs. the value of previous age. J-T p values indicate the significance of trends with age for each parameter analyzed with Jonckheere-Terpstra test (trend test); significance at $p < 0.05$

the heights of the PZ and HZ begin to decline after PD40, particularly by PD60, pointing to decreased proliferation and activity of the chondrocytes (Fig. 2).

Coordinated osteoblast activity and mineralization in the lower HZ forms the 1° Sn, which is located under the GP and characterized by thin trabeculae with a calcified cartilage core covered with bone (Hunziker and Schenk 1989). During growth, the calcified cartilage is replaced by lamellar bone, and forms the 2° Sn (Kimmel and Jee 1980). So far, there have been few detailed reports about changes in the height of the Sn during puberty. Here we showed that the height of whole Sn was little changed by PD40 but that it increased by PD50, mainly due to a marked increase in the 2° Sn (Figs. 2 and 4). The constant height of the whole Sn up to PD40 may be a reflection of a relatively constant rate of osteoblast activity or mineralization in the lower HZ. On the other hand, a dramatic increase of 2° Sn height at PD50 was accompanied by increases in parameters related to bone formation, such as bone area, bone area ratio, number of trabeculae and bone perimeter (Fig. 2, Table 1), and the increase of the 2° Sn at PD50 seemed to be associated with a significant decrease in the HZ over the same period. The architecture of the tibial epiphysis changes with age, with a significant increase of bone area ratio and trabecular thickness and, as a consequence, reduced trabecular separation. As shown in Fig. 4, the increased trabecular width and gradually reduced trabecular number except at PD50 result in time in more widely separated and thickened trabeculae.

Longitudinal bone growth during puberty is controlled by a complex endocrine system. In particular, IGF-1 is a potent stimulator of longitudinal bone growth during puberty (Venken et al. 2007). Since IGF-1 can stimulate proliferation of chondrocytes (Ohlsson et al. 1992), the sudden increase in IGF-1 levels at PD30 should contribute to the parallel increase in the PZ (Fig. 5A). However, the cell numbers and height of the PZ at PD30 were lower than at PD20 (Fig. 2C). This discrepancy may be the result of the rapid transition of proliferating cells into hypertrophic cells. In addition to IGF-1, a number of clinical and experimental studies demonstrate that estrogen also provides an important stimulus for long bone growth during puberty (Cutler 1997; Vanderschueren et al. 1997; Vidal et al. 2000). Serum estradiol levels showed considerable variation between individuals and gradually decreased with age (Fig. 5B). There are conflicting

results concerning the ability of estrogen to stimulate long bone growth, depending on the level of estrogen: low levels of estrogen caused maximal stimulation of epiphyseal growth, whereas high levels caused opposing effects (Cutler 1997). These results suggest that a specific level of E_2 may be needed for optimal regulation of long bone growth during puberty. Testosterone is also important for bone growth during puberty (Venken et al. 2007). We noted a rise of T levels after PD30 in the male rats (Fig. 5C). Although the effect of androgens depends on their conversion into estrogens (Vanderschueren et al. 1997; Vidal et al. 2000), androgens by themselves appear to stimulate long bone growth (Keenan et al. 1993). Consistent with this, T levels rose steeply without altering E_2 levels, and then gradually decreased (Fig. 5C). Considering that androgens can directly stimulate chondrocyte proliferation (Krohn et al. 2003) and bone mineralization (Krabbe et al. 1979), the sudden increases in T level may participate in promoting longitudinal growth, as well as mineral acquisition after PD40, when IGF-1 levels are going down.

Our comprehensive data provide normative information concerning developmental changes in bone density of long bones, histomorphometry of the tibial GP, and hormones relevant to long bone growth during puberty in the rat. This will be useful for planning animal toxicological studies, especially in reducing animal numbers by determining the appropriate age and number of animals to use in given experiments.

Supplementary Information The online version contains supplementary material available at https://doi.org/10.1007/s12565-024-00766-6.

Acknowledgements KR and OL participated in data analysis, experimental work and development of the manuscript, and JR participated in the design of the study, data analysis, and supervision. JR takes responsibility for the integrity of the data analysis. All authors read and approved the final manuscript. This work was supported by the Basic Science Research Program through the National Research Foundation of Korea (NRF) funded by the Ministry of Education and Science [NRF-2022R1F1A1069408].

Declarations

Conflict of interest All authors state that they have no conflicts of interest with any financial organization regarding the material discussed in the manuscript.

Data availability The authors confirm that the data supporting the findings of this study are available within the article and its supplemental files.

References

Börjesson AE, Lagerquist MK, Liu C et al (2010) The role of estrogen receptor α in growth plate cartilage for longitudinal bone growth. J Bone Miner Res 25:2690–2700

Choi Y, Choi Y, Kim J, Choi H, Shin J, Roh J (2016) Peripubertal caffeine exposure impairs longitudinal bone growth in immature male rats in a dose-and time-dependent manner. J Med Food 19:73–84

Cutler GB Jr (1997) The role of estrogen in bone growth and maturation during childhood and adolescence. J Steroid Biochem Mol Biol 61:141–144

Engelbregt M, Tromp A, van Lingen A, Popp-Snijders C, Delemarre-van de Waal HA (1999) Validation of whole body DXA in young and adult rats. Horm Res 51(suppl 2):428

Gluckman PD, Hanson MA (2006) Evolution, development and timing of puberty. Trends Endocrinol Metab 17(1):7–12

Hansson L, Menander-Sellman K, Stenström A, Thorngren KG (1972) Rate of normal longitudinal bone growth in the rat. Calcif Tissue Res 10(3):238–251

Hunziker E, Schenk R (1989) Physiological mechanisms adopted by chondrocytes in regulating longitudinal bone growth in rats. J Physiol 414:55–71

Hunziker EB (1994) Mechanism of longitudinal bone growth and its regulation by growth plate chondrocytes. Microsc Res Tech 28(6):505–519

Keenan BS, Richards GE, Ponder SW, Dallas JS, Nagamani M, Smith ER (1993) Androgen-stimulated pubertal growth, the effects of testosterone and dihydrotestosterone on growth hormone and insulin-like growth factor-I in the treatment of short stature and delayed puberty. J Clin Endocrinol Metab 76(4):996–1001

Kember NF (1983) Cell kinetics of cartilage. In: Hall B K (ed) Cartilage Vol. 1, Academic Press, New York, pp 149–179

Kimmel DB, Jee WS (1980) Bone cell kinetics during longitudinal bone growth in the rat. Calcif Tissue Int 32(2):123–133

Krabbe S, Christiansen C, Rødbro P, Transbøl I (1979) Effect of puberty on rates of bone growth and mineralisation: with observations in male delayed puberty. Arch Dis Child 54(12):950–953

Krohn K, Haffner D, Hügel U, Himmele R, Klaus G, Mehls O, Schaefer F (2003) 1,25(OH)2D3 and dihydrotestosterone interact to regulate proliferation and differentiation of epiphyseal chondrocytes. Calcif Tissue Int 73(4):400–410

Lindahl O (1967) The rigidity of fracture immobilization with plates. Acta Orthop Scand 38(1):101–114

Ohlsson C, Nilsson A, Isaksson O, Lindahl A (1992) Growth hormone induces multiplication of the slowly cycling germinal cells of the rat tibiael growth plate. Proc Natl Acad Sci U S A 89(20):9826–9830

Ortega N, Behonick DJ, Werb Z (2004) Matrix remodeling during endochondral ossification. Trends Cell Biol 14(2):86–93

Parfitt AM, Drezner MK, Glorieux FH et al (1987) Bone histomorphometry, standardization of nomenclature, symbols, and units. Report of the ASBMR Histomorphometry Nomenclature Committee. J Bone Miner Res 2(6):595–610

Roach HI, Mehta G, Oreffo RO, Clarke NM, Cooper C (2003) Temporal analysis of rat growth plates: cessation of growth with age despite presence of a physis. J Histochem Cytochem 51(3):373–383

Staines K, Pollard AS, McGonnell IM, Farquharson C, Pitsillides AA (2013) Cartilage to bone transitions in health and disease. J Endocrinol 219(1):R1–R12

Theintz G, Buchs B, Rizzoli R et al (1992) Longitudinal monitoring of bone mass accumulation in healthy adolescents, evidence for a marked reduction after 16 years of age at the levels of lumbar spine and femoral neck in female subjects. J Clin Endocrinol Metab 75(4):1060–1065

Vanderschueren E, van Herck E, Nijs J, Ederveen AG, De Coster R, Bouillon R (1997) Aromatase inhibition impairs skeletal modeling and decreases bone mineral density in growing male rats. Endocrinology 138(6):2301–2307

Venken K, Movérare-Skrtic S, Kopchick JJ et al (2007) Impact of androgens, growth hormone, and IGF-I on bone and muscle in male mice during puberty. J Bone Miner Res 22(1):72–82

Vidal O, Lindberg MK, Hollberg K et al (2000) Estrogen receptor specificity in the regulation of skeletal growth and maturation in male mice. Proc Natl Acad Sci U S A 97(10):5474–5479

Walker KV, Kember NF (1972) Cell kinetics of growth cartilage in the rat tibiae. II. Measurements during ageing. Cell Tissue Kinet 5(5):409–419

Waynforth HB, Flecknell PA (1980) Reproductive parameters and organ weights: Experimental and surgical technique in the rat, 2nd ed. Academic Press, London, pp 346 (Vol. 127)

Weinreb M, Rodan GA, Thompson DD (1991) Depression of osteoblastic activity in immobilized limbs of suckling rats. J Bone Miner Res 6(7):725–731

Weise M, De-Levi S, Barnes KM, Gafni RI, Abad V, Baron J (2001) Effects of estrogen on growth plate senescence and epiphyseal fusion. Proc Natl Acad Sci U S A 98(12):6871–6876

Wheeler MD (1991) Physical changes of puberty. Endocrinol Metab Clin North Am 20:1–14

Wilsman NJ, Leiferman EM, Fry M, Farnum CE, Barreto C (1996) Differential growth by growth plates as a function of multiple parameters of chondrocytic kinetics. J Orthop Res 14(6):927–936

Zoetis T, Tassinari MS, Bagi C, Walthall K, Hurtt ME (2003) Species comparison of postnatal bone growth and development. Birth Defects Res B Dev Reprod Toxicol 68(2):86–110